Single-Cell RNA Sequencing Reveals Heterogeneity Among Adult Mouse, Primate and Human Kidney Cells

Shuai Chen (cs496923026@163.com)
Guangxi Medical University
Jinling Liao
Guangxi Medical University
Yang Chen
Guangxi Medical University
Yufang Lv
Guangxi Medical University
Qiong Song
Guangxi Medical University
Lihui Wang
Guangxi Medical University
Chao Huang
Guangxi Medical University
Xin Yang
Guangxi Medical University
Kechen Du
Guangxi Medical University
Zengnan Mo
Guangxi Medical University
Chunlin Zou
Guangxi Medical University

Article

Keywords: Nonhuman primates, kidney, single cell RNA sequencing, across species

Posted Date: January 7th, 2022

DOI: https://doi.org/10.21203/rs.3.rs-1207698/v1

Abstract

Multiple studies have been performed to map the kidney landscape of human and rodent, along with the development of sequencing technique. Although rodent disease models have been widely applied, many disadvantages also exist. Non-human primates (NHPs) are considered as the closest experimental animals to humans and show great advantages in the construction of animal models of human disease. Therefore, a comprehensive understanding of the heterogeneity and homogeneity between human and multiple animal kidney cells is important for further establishing animal models of human renal disease. Here, we generated the first single-cell transcriptome data of normal adult cynomolgus monkey kidney using 10x Genomics scRNA-seq platform. Then, we further performed an in-depth comparison across species at the single-cell level, and our analysis indicated that the gene expression of adult primate kidney cells showed a better correlation with human kidney than mouse kidney. Furthermore, our results demonstrated that the cellular localization of GWAS-identified renal disease genes showed differences across species. The cellular localization of blood pressure associated genes in human displayed similarity to cynomolgus monkey. This study provided a reliable reference for further studies associated with renal diseases on NHPs. In addition, our results also provided a novel insight into the choice of renal disease animal model and a detailed explanation for close genetic relationship between NHPs and human at a single cell level.

Background

The kidney is a complex and important organ which perform diverse physiological functions that are essential for health [1]. Nephron is the functional units of adult kidney. An adult human has about 1 million nephrons per kidney [2], and each nephron is composed of two parts, the renal corpuscle and the renal tubule. The renal corpuscle contains glomerulus and Bowman's capsule, and the renal tubule includes proximal tubule (PT), medullary loop and distal tubule (DT). The reciprocal coordination and complementary interactions of renal corpuscle, renal tubules and collecting duct filter initial urine from the blood, reabsorb water and nutrients, and secrete wastes, producing the final urine, which is expelled [3,4].

A detailed cellular anatomical description of kidney is vital to address the pathogenic and pathological mechanism of renal diseases, including renal cancer. With the development of next-generation sequencing technology, high-throughput single-cell analysis [5,6] and the Human Cell Atlas [7,8], multiple studies have been carried out to map the adult human and rodents kidney landscape [9–13]. Park et al. characterized 57,979 cells from healthy mouse kidney using single cell RNA sequencing (scRNAseq) and highlighted cell-type specific cellular targets of kidney diseases [9]. Zimmerman et al. filtered 3013, 3935, 4671 and 2868 $CD45^+$ immune cells from mouse, rat, pig, and human kidney tissues, respectively. Further analysis identified a conserved population of innate immune cells across multiple species, and screened out potential cell markers for future studies of this candidate resident macrophage population in mouse, rat and pig [14]. However, there is few report about single cell transcriptome profiling of nonhuman

primates (NHPs) [15–20]. The comparison of transcriptome profiles between human, NHPs and other animal species at single cell resolution had not been reported.

The nonhuman primate has been considered as important translational model that bridge the gap between laboratory research to clinical application. As early as in 1960s, Feldman et al. reported a rhesus monkey model of nephrotic syndrome with glomerulonephritis [21]. Liu et al. successfully established type 1 diabetic mellitus NHPs models via partial pancreatectomy and low-dose streptozotocin (STZ) administration, which were further induced to diabetic nephropathy (DN) models by long-term effects of hyperglycemia [22–24]. The DN monkeys showed a distinct metabolic disturbance which were similar to DN patients, including higher levels of VLDL/LDL, lipids, unsaturated lipids, uric acid, fumarate and hippurate, as well as lower levels of HDL, alanine, glutamate and NAD^+. More importantly, the DN monkeys exhibited obvious glomerulosclerosis and tubulointerstitial lesions, which was consistent with previous reports about chronic renal injury in diabetic patients [24,25]. By means of intravenous administration of cisplatin, Moghadasali et al. induced acute kidney injury (AKI) and chronic kidney disease (CKD) in adult cynomolgus monkey [26,27]. Four days after injections of cisplatin, creatinine and urea levels were found to be significantly increased in treated monkeys in comparison with normal monkeys. The pathological changes of renal tubules in AKI monkeys showed cytoplasmic vacuolization, loss of brush border, epithelial cell detachment in addition to luminal cell debris and nuclear fragmentation, which appeared to better mimic human nephropathy [26]. Furthermore, the treated monkeys exhibited obvious pathological changes of CKD, including tubular loss, glomerular fibrosis and cortical fibrosis after long-term administration of cisplatin. [27].

Using scRNA-seq, we constructed a single cell atlas of healthy adult cynomolgus monkey kidney and identify distinct types of kidney cells. Moreover, we demonstrate different gene expression profiles across species at a single cell resolution and annotate the gene expression of complex traits disease in human, monkey and mouse. Our study will provide an experiment basis for establishing animal models of renal disease.

Materials And Methods

Animals and ethics statement

One adult male and two adult female (10-12 years old) cynomolgus monkeys were raised at Wincon TheraCells Biotechnologies Co.Ltd (Guangxi, China), which is a non-human primate research facility accredited by AAALAC. The experimental protocols were approved by Institutional Animal Care and Use Committee of the Wincon TheraCells Biotechnologies. All animal experiments were conducted by certified veterinarians, according to the approved guidelines.

Preparation of single cell suspension from monkey kidney

To ensure the vitality of kidney tissues, three kidney tissue samples were harvested separately from three monkeys at different days. In brief, the monkeys were anesthetized with pentobarbital sodium (50mg/kg, iv), and then the left kidney was removed from the abdomen cavity and immediately immersion placed in ice-cold RPMI 1640 (WISENT, 350-006-CL) supplemented with 5% Fetal bovine serum (FBS, Gibco, 10099-141C) and 1% Antibiotic-Antimycotic (Gibco, 15240062). Then, the renal capsule was removed, and 0.5g of full-thickness kidney tissue were cut off using surgical scissors. After washing with 4℃ Dulbecco's phosphate-buffered saline (DPBS, WISENT, 311-425-CL) twice, the tissue was placed into a 60 mm cell culture dish containing DPBS and minced into 1 mm^3 pieces using micro scissors on ice. Subsequently, we collected the kidney tissue fragments into the centrifuge tube and centrifuged at 300 rpm for 3 minutes at 4℃. After discarding the supernatant, we used 10mL RPMI 1640 containing 0.1mg/ml Liberase TL (Roche, 05401020001) and 0.1 mg/ml DNase Ⅰ to digest the kidney tissue fragments for 40 min at 37℃. Digestion was terminated by RPMI 1640 containing 10% FBS. The cell suspension were then filtered through a 70 μm cell strainer and centrifuged at 300 rpm for 5min at 4℃. After discarding the supernatant, the red blood cells were removed by treating with RBC lysis buffer (Roche, 11814389001) for 5 minutes. The cells were then spun down and re-suspended in DPBS. After the supernatant was poured off, the cells were re-suspended in DPBS and filtered through a 40 μm cell strainer. The number of live cells were counted using trypan blue staining (Gibco, 420301).

Single-cell RNA library construction and squencing

The Chromium Single Cell 3' GEM, Library&Gel Bead Kit v3 (10X Genomics, 1000075) and Chromium Chip B Single Cell Kit (10X Genomics, 1000153) was used for single-cell RNA library preparation. The single cells were resuspended in PBS with 0.1% BSA to around 700-1000 cells per milliliter. Then, the cell suspension, Gel Bead and Partitioning Oil were dispensed into the Chromium Single-Cell B Chip, and the assembled chip was placed onto a Chromium Controller (10× Genomics) to generate single-cell Gel Bead-In-EMulsions (GEMs). GEM-reverse transcription (RT) was conducted using a T100 Termal Cycler (Bio-Rad). After RT, cDNA was recovered using Recovery Agent and then cleaned up using the Dynabeads Cleanup Mix. Subsequently, cDNA was amplified using a T100 Termal Cycler. The amplified cDNA product was cleaned up with SPRIselect Reagent Kit. Indexed sequencing libraries were constructed using Chromium Single Cell 3' Reagent Kit v3. Library quality was checked by the Agilent 2100 Bioanalyzer (performed by Genery Biotechnology, Shanghai). All libraries were sequenced on the Illumina Nova S6000 (performed by Genery Biotechnology, Shanghai).

scRNA-seq raw data processing

Preliminary sequencing results (bcl files) were converted to FASTQ files with CellRanger (version 3.0, http://10xgenomics.com). The FASTQ files were then aligned to the cynomolgus monkey genome reference sequence, Macaca_fascicularis_5.0. Meanwhile, we also generated a file containing a barcodes table, a genes table, and a gene expression matrix using Cell Ranger. Next, we obtained an overview website containing a considerable amount of information, such as number of cells, median number of detected genes and others.

Quality control (QC) and monkey kidney data second analysis

We used the R (version 4.0.0, https://www.r-project.org/) and Seurat R package (version 3.0, https://satijalab.org/seurat/). Cells with <200 and >4000 genes (potential doublets) and a mitochondrial gene percentage of >50% were removed. After QC, 28019 high quality kidney cells were obtained.

Due to these samples were obtained from three cynomolgus monkey and sequenced in batches, NHPs IDs were used to eliminate potential batch effect. After data normalization, we identified top 2000 variable genes and created potential Anchors with FindIntegrationAnchors function of Seurat. Then, IntegrateData function was used to integrate data and create a new matrix with 2000 features, in which potential batch effect was regressed out. We then used principal-component analysis (PCA), with the variable genes as input, and identified significant principal components based on the jackStraw function. A total of 20 PCs were used to perform the downstream analysis. The cell clusters were identified by FindCluster function with a resolution of 0.2 and then were visualized with 2D UMAP plots. Next, we find differentially expressed genes (DEGs) between each type of cells using FindAllMarkers function.

Human and mouse data from NCBI were analyzed using a similar method. NCBI data available from the Gene Expression Omnibus (GEO) and Sequence Read Archive (SRA), accession GSE131685, GSE107585, SRR6348586, SRR6348583, SRR6348584 and GSE141115.

Gene expression comparison cross-species

For species-based profile analysis, we first transferred the cynomolgus monkey and mouse gene names into human homologous gene names with the ENSEMBL R package BioMart (version 2.44.4, http://www.biomart.org/). We discarded genes with no gene names and retained identical names between the human and mouse, human and cynomolgus monkey kidney database. Correlation coefficients between human and cynomolgus monkey, and between human and mouse kidney database were calculated, and regression curves were plotted via scatter diagram using ggplot2 package. Subsequently, we used the Subset function of Seurat to select mutual types of cell among human, monkey and mouse kidney database, and performed correlation analysis with a similar method.

Based on the average expression of homologous genes, we used pheatmap package to plot heatmap for the expression of complex traits kidney diseases related genes across species. Next, the expression of target genes related to hypertension therapy were plotted using Vlnplot function.

Results

scRNAseq profiling and clustering of adult cynomolgus monkey kidney cells

We sorted and sequenced a total of 43,899 cells from kidney cell suspensions from one male and two female adult healthy cynomolgus monkey. After stringent quality control, 28,019 high-quality cells were retained for further analysis. The initial UMAP analysis revealed 37 cell clusters (Additional file Fig. 1A). Based on cell-specific markers, we identified each cell clusters unbiasedly. For example, based on the markers *LRP2*, *ALDOB* and *MT1G*, we identified cluster 0-2, 4, 7-8, 14-18, 20 and 26 cells as proximal tubule cells [8,28,29]. Cluster 5, 11 and 29 cells expressed high levels of *EMCN* and *IGFBP5*, which are well accepted as molecular markers for endothelium [30]. Similarly, cluster 6 and 28 cells were identified as intercalated cells and principle cells respectively according to *ATP6V0D2*, *SPINK1*, *ATP6V1G3* and *FXYD4* [31]. Finally, our single kidney cell profiling revealed 11 distinct cell types, including proximal tubule cells, endothelium, intercalated cells, principle cells, loop of Henle, distal tubule cells, T/NK cells, B cells, macrophages, myofibroblasts and a small cluster of erythroid cells. (Fig. 1A, 1B)

Integrating and clustering of human and mouse kidney scRNAseq database

To gain a better comparison of the scRNAseq transcriptomic profiles of kidney across species, we integrated four healthy human and thirteen healthy mouse kidney scRNAseq database respectively by finding 'anchors' among different datasets [32]. After quality control, 44,795 human kidney cells and 64,966 mouse kidney cells were retained for downstream comparison. We identified 31 cell clusters representing 9 distinct cell types through scHCL analysis on integrated human database (Fig. 1B, 1D, Additional file Fig. 1B). Cluster 22 cells were identified as loop of Henle, which expressed high levels of *UMOD* and *SLC12A1* [33,34], although they also expressed low levels of distal tubule cells specific markers (*CALB1* and *SLC12A3*). We could not define myofibroblasts and podocytes due to the low expression levels of *ACTA2*, *MYL9*, *TAGLN* and *NPHS2* within all clusters.

Integrated mouse database was identified into 28 cell clusters and 11 cell types. Podocytes were identified clearly according to the expression of *Nphs2* and *Cdkn1c* [9]. (Fig. 1C, 1F, Additional file Fig. 1C)

Correlation analysis of kidney cells across species at single-cell level

We calculated the average gene expression of all cells in three databases within mutual clusters across species. cynomolgus monkey and mouse gene names were transferred into human homologous gene names using R package biomaRt [35]. Finally, 12,993 homologous genes derived from cynomolgus monkey database and 13,056 homologous genes derived from mouse database were retained for downstream analysis.

First, we compared the expression of all homologous genes between human and monkey kidney cells, as well as between human and mouse kidney cells (Fig. 2A, 2B). The Pearson correlation coefficients were 0.806 and 0.778, respectively (Fig. 2C, 2D). Some genes, such as *DHDH*, *MT3* and *FUOM* were highly expressed in human kidney cells, but showed low expression in kidney cells from cynomolgus monkey. On the contrary, *IGFBP5*, *FUOM* and *GPX3* were highly expressed in monkey kidney cells, but is low in human kidney cells (Fig. 2C, Additional file Data1). The expression of *CRYAB*, *RPL35* and *GAPDH* were

lower in mouse kidney cells than human kidney cells. *KLK1*, *SLC34A1* and *FXYD6-FXYD4* were highly expressed in mouse kidney cells, but is low in human kidney cells (Fig. 2D, Additional file Data1).

Next, we analyzed all cell types in these three species and found that some cynomolgus monkey and human kidney cells were well correlated. Of all these cells, high correlations were observed between cynomolgus monkey and human PT cells, endothelium, and T cells, the Pearson correlation coefficients were 0.838, 0.824 and 0.836 respectively. Similarly, we observed high correlations between mouse and human PCs and B cells, the Pearson correlation coefficients were 0.794 and 0.815, respectively (Additional file Fig. 2). Interestingly, we also noticed that cynomolgus monkey and mouse macrophages showed well correlation with human neutrophils, the Pearson correlation coefficients were 0.84 and 0.814, respectively. Furthermore, we identified species-specific and shared DEGs of these high correlated cells (HCCs) in cynomolgus monkey, human and mouse kidney. For example, between cynomolgus monkey and human specific markers, *B2M*, *SPP1* and *GPX3* were specifically expressed in human PT cells. In contrast, these genes were poorly expressed in cynomolgus monkey. On the contrary, *MT3*, *FUOM* and *DHDH* were specifically expressed in cynomolgus monkey PT cells (Fig. 2E). In addition, *ALDOB*, *PFDN1* and *RARRES2* were expressed in both human and cynomolgus monkey (Additional file Data1).

To investigate the correlation of different subtypes of high correlated cells clusters among different species, we used Seurat SubsetData function to select the PT cells, endothelium and T cells in both human and cynomolgus monkey as well as B cells and PCs in both human and mouse databases, and performed re-clustering respectively. Further correlation analyses were conducted based on these subsets of HCCs. We found that most subsets of HCCs were relatively well correlated, but heterogeneity still exists.

Poor correlations were observed between PT18 cells in cynomolgus monkey kidney and all the subtypes of PT cells in human kidney (Fig. 2F).

Complex trait disease genes show heterogeneity of cell-type specificity across species

A previous study had demonstrated that that hereditary kidney disease-related genes showed cell-type specificity in mouse kidney. However, there are very few similar studies in human and nonhuman primates. Therefore, we annotated the expression of complex trait disease genes that have been associated with chronic kidney disease (CKD), systemic lupus erythematosus (SLE), serum metabolite levels and blood pressure (BP) in human, cynomolgus monkey and mouse kidney cells (Fig. 3A-D). Our result indicated that most genes involved in these complex trait diseases show a similar cell type-specific expression pattern in the three species, but differences were also observed across species. For example, the expression of some genes associated with CKD was mainly specified in human PT cells, endothelium and PCs, whereas these genes were mainly expressed in cynomolgus monkey PT cells and ICs and in mouse PT cells, PCs and podocytes. The genes associated with serum metabolite levels such as *SLC17A3*, *BHMT* and *SLC7A9* showed strong enrichment for PT cells. Besides, we noticed that other genes associated with serum metabolite levels were also highly expressed in PCs, endothelium and aLOH of human kidney, but similar results were not observed in cynomolgus monkey and mouse kidney cells.

Among all of the genes related to complex trait diseases, the genes associated with blood pressure exhibited significant different expression patterns across species. Previous study has demonstrated that BP-associated genes were mostly expressed in mouse collecting duct cells (including ICs and PCs). In our integrated mouse database, the expression of BP-associated genes also showed enrichment for cell types of myofibroblasts, podocytes and macrophages. However, the BP-associated genes showed very high expression in PT cells, collecting duct cells and endothelium in human and cynomolgus monkey although they are also expressed in myofibroblasts in cynomolgus monkey. Furthermore, we found that the expression of genes of the renin-angiotensin system (including *ACE*, *ACE2*, *MME*, *ECE1*, *AGTR1*, *AGTR2* and *MAS1*) displayed species differences (Fig. 4A-C). For example, the expression of *AGTR1* and *AGTR2* were not found in human kidney. Meanwhile, the expression of *AGTR2* and *MAS1* were not found in cynomolgus monkey kidney and the expression of *Agtr2a* was not found in mouse kidney. The expression of *MME* was mainly in PT cells of human and cynomolgus monkey kidney, whereas *Mme* were expressed in PT cells, aLOH and ICs in mouse kidney. Our single cell transcriptome analysis will provide valuable information to establishing animal model of kidney disease.

Discussion

Nonhuman primates (NHPs) play an important role in the establishment of disease models due to their similarity to humans in physiology, anatomy, immunology and genetics. For a half century, NHPs have been widely used in biomedical research. There has been a relative increase in the importance and advantage of using NHPs as pre-clinical models in infectious diseases [36,37], ageing-related and neurological disorders [38,39], endocrine diseases [40,41] and others. Nevertheless, the differences between human and NHPs should not be neglected, and more efforts need to be done to distinguish the cellular and genetic differences between NHPs and human.

Here, we provide a molecular definition of cell types in normal adult cynomolgus monkey kidney by single-cell RNA-sequencing of 43,899 cells. In the current study, scRNAseq data revealed 11 distinct cell types by quantitative gene expression, including PT cells, endothelium, ICs, PCs, aLOH, DT, myofibroblasts, three types of immune cells (NKT cells, macrophages and B cells) and a small cluster of erythroid cells, and these cells included almost all previously described cell types in human and rodent kidney [8–10]. Our work complements the deficiency of the research on single-cell transcriptome atlas of NHPs and provides a reference for future investigations of NHPs kidney cells as well as for studies on kidney diseases in NHPs at single cell resolution.

Our scRNAseq data also provides novel insights into the correlation between NHPs and human kidney cells. We demonstrated that transcriptome of human kidney was more closely correlated with that of nonhuman primate kidney than that of mouse kidney. The gene expression of PT cells, endothelium and ICs in cynomolgus monkey kidney showed the highest correlation with gene expression of these cells in human kidney. Previous study revealed the sex diversity in human and mouse renal PT cells as well as a shared and species-specific differential gene expression between human and mouse PT cells [42]. In our study, we performed a correlation analysis of PT cells and subsets of PT cells across species. The result

demonstrated that PT cells and most of the subtypes of PT cells in cynomolgus monkey kidney were well correlated with those cells in human kidney. Interestingly, we noticed that a specific subtype of PT cells in cynomolgus monkey kidney showed a low correlation with all of the subtypes of PT cells in human kidney. The function of this cluster of PT cells in cynomolgus monkey kidney needs further investigation. In short, this is the first time that reveal the similarities and differences between human and monkey kidney cells at a single cell level.

Park et al. has demonstrated that the expression of kidney disease-associated genes is restricted to specific kidney cell types [9]. In this study, we applied a similar approach to the analysis of the relation between human and monkey kidney cells and kidney diseases. Our results revealed the heterogeneity of the expression of complex trait kidney disease associated genes across species. Genes associated with plasma metabolite are predominantly expressed in human PT cells, endothelium and PCs, However, PCs and endothelium shows low enrichment for metabolite related genes in monkey and mouse. Additionally, we noticed that BP-associated genes also highly expressed in human and monkey PT cells and endothelium, whereas the previous study in mouse kidney demonstrated these genes were mainly expressed in collecting duct cells. Therapeutic target genes for hypertension also showed significant differences across species. For example, MME highly enriched in PT cell of human and cynomolgus monkey kidney, whereas it was widely expressed in PT cells, ICs, aLOH and podocytes in mouse kidney.

In summary, we generates the first single-cell transcriptomic atlas of the adult primate kidney and uncovers across-species differences in kidney gene expression at single-cell level. This study will improve our understanding of primate kidney biology. Furthermore, the data in this study will also provide useful information for the establishment of animal models of various renal disease in different species and provides a foundation for future studies.

Declarations

Authors' Contributions

J.L. and Y.L. performed RNA-seq experiments, made cDNA library; S.C. performed single-cell RNA-seq analyses, made figures, and wrote the paper; Y.C. wrote the paper; C.Z. and J.L. dissected monkey kidney tissues, performed RNA-seq experiments; Q.S. and L.W. discussed the draft paper, and critically reviewed the manuscript; C.H. and K.D. offered bioinformatics help. Z.C. and Z.M. conceived of and supervised the project, analyzed data, made figures, and wrote the paper; and all authors read and commented on the manuscript.

Competing Interests

The authors declare that they have no competing interests.

Funding

This work was supported by the National Natural Science Foundation of China (81670750, 81770759, 81971191 and 81360123), Major Project of Guangxi Innovation Driven (AA18118016), National Key Research and Development Program of China (2017YFC0908000), Guangxi key Laboratory for Genomic and Personalized Medicine (grant number 16-380-54, 17-259-45, 19-050-22, 19-185-33, 20-065-330).

Author details

[1]Key Laboratory of Longevity and Ageing-Related Disease of Chinese Ministry of Education, Center for Translational Medicine and School of Preclinical Medicine, Guangxi Medical University, 530021, Nanning, Guangxi, China. [2]Center for Genomic and Personalized Medicine, Guangxi Medical University, 530021, Nanning, Guangxi, China.

Data availability

Raw data for single-cell RNA-seq will further uploaded in NCBI database.

References

1 McMahon A. P. Development of the Mammalian Kidney. *Curr Top Dev Biol***117**, 31-64, doi:10.1016/bs.ctdb.2015.10.010 (2016).

2 Kramer H. Diet and Chronic Kidney Disease. *Adv Nutr***10**, S367-S379, doi:10.1093/advances/nmz011 (2019).

3 Curthoys N. P. & Moe O. W. Proximal tubule function and response to acidosis. *Clin J Am Soc Nephrol***9**, 1627-1638, doi:10.2215/CJN.10391012 (2014).

4 Subramanya A. R. & Ellison D. H. Distal convoluted tubule. *Clin J Am Soc Nephrol***9**, 2147-2163, doi:10.2215/CJN.05920613 (2014).

5 Macosko E. Z., Basu A., Satija R., Nemesh J., Shekhar K., Goldman M. *et al.* Highly Parallel Genome-wide Expression Profiling of Individual Cells Using Nanoliter Droplets. *Cell***161**, 1202-1214, doi:10.1016/j.cell.2015.05.002 (2015).

6 Tang F., Barbacioru C., Wang Y., Nordman E., Lee C., Xu N. *et al.* mRNA-Seq whole-transcriptome analysis of a single cell. *Nat Methods***6**, 377-382, doi:10.1038/nmeth.1315 (2009).

7 Regev A., Teichmann S. A., Lander E. S., Amit I., Benoist C., Birney E. *et al.* The Human Cell Atlas. *Elife***6**, doi:10.7554/eLife.27041 (2017).

8 Han X., Zhou Z., Fei L., Sun H., Wang R., Chen Y. *et al.* Construction of a human cell landscape at single-cell level. *Nature***581**, 303-309, doi:10.1038/s41586-020-2157-4 (2020).

9 Park J., Shrestha R., Qiu C., Kondo A., Huang S., Werth M. *et al.* Single-cell transcriptomics of the mouse kidney reveals potential cellular targets of kidney disease. *Science***360**, 758-763, doi:10.1126/science.aar2131 (2018).

10 Liao J., Yu Z., Chen Y., Bao M., Zou C., Zhang H. *et al.* Single-cell RNA sequencing of human kidney. *Sci Data***7**, 4, doi:10.1038/s41597-019-0351-8 (2020).

11 Wu H., Malone A. F., Donnelly E. L., Kirita Y., Uchimura K., Ramakrishnan S. M. *et al.* Single-Cell Transcriptomics of a Human Kidney Allograft Biopsy Specimen Defines a Diverse Inflammatory Response. *J Am Soc Nephrol***29**, 2069-2080, doi:10.1681/ASN.2018020125 (2018).

12 Wang P., Chen Y., Yong J., Cui Y., Wang R., Wen L. *et al.* Dissecting the Global Dynamic Molecular Profiles of Human Fetal Kidney Development by Single-Cell RNA Sequencing. *Cell Rep***24**, 3554-3567 e3553, doi:10.1016/j.celrep.2018.08.056 (2018).

13 Denisenko E., Guo B. B., Jones M., Hou R., de Kock L., Lassmann T. *et al.* Systematic assessment of tissue dissociation and storage biases in single-cell and single-nucleus RNA-seq workflows. *Genome Biol***21**, 130, doi:10.1186/s13059-020-02048-6 (2020).

14 Zimmerman K. A., Bentley M. R., Lever J. M., Li Z., Crossman D. K., Song C. J. *et al.* Single-Cell RNA Sequencing Identifies Candidate Renal Resident Macrophage Gene Expression Signatures across Species. *J Am Soc Nephrol***30**, 767-781, doi:10.1681/ASN.2018090931 (2019).

15 Yi W., Lu Y., Zhong S., Zhang M., Sun L., Dong H. *et al.* A single-cell transcriptome atlas of the aging human and macaque retina. *National Science Review*, doi:10.1093/nsr/nwaa179 (2020).

16 Wang S., Zheng Y., Li J., Yu Y., Zhang W., Song M. *et al.* Single-Cell Transcriptomic Atlas of Primate Ovarian Aging. *Cell***180**, 585-600 e519, doi:10.1016/j.cell.2020.01.009 (2020).

17 Peng Y. R., Shekhar K., Yan W., Herrmann D., Sappington A., Bryman G. S. *et al.* Molecular Classification and Comparative Taxonomics of Foveal and Peripheral Cells in Primate Retina. *Cell***176**, 1222-1237 e1222, doi:10.1016/j.cell.2019.01.004 (2019).

18 Zhang W., Zhang S., Yan P., Ren J., Song M., Li J. *et al.* A single-cell transcriptomic landscape of primate arterial aging. *Nat Commun***11**, 2202, doi:10.1038/s41467-020-15997-0 (2020).

19 Zhu Y., Sousa A. M. M., Gao T., Skarica M., Li M., Santpere G. *et al.* Spatiotemporal transcriptomic divergence across human and macaque brain development. *Science***362**, doi:10.1126/science.aat8077 (2018).

20 Daughtry B. L., Rosenkrantz J. L., Lazar N. H., Fei S. S., Redmayne N., Torkenczy K. A. *et al.* Single-cell sequencing of primate preimplantation embryos reveals chromosome elimination via cellular fragmentation and blastomere exclusion. *Genome Res***29**, 367-382, doi:10.1101/gr.239830.118 (2019).

21 Feldman D. B. & Bree M. M. The nephrotic syndrome associated with glomerulonephritis in a rhesus monkey (Macaca mulatta). *J Am Vet Med Assoc***155**, 1249-1252 (1969).

22 Qiao C. F., Tian B. L., Mai G., Wei L. L., Jin X., Ren Y. *et al.* Induction of diabetes in rhesus monkeys and establishment of insulin administration strategy. *Transplant Proc***41**, 413-417, doi:10.1016/j.transproceed.2008.08.144 (2009).

23 Wei L., Lu Y., He S., Jin X., Zeng L., Zhang S. *et al.* Induction of diabetes with signs of autoimmunity in primates by the injection of multiple-low-dose streptozotocin. *Biochem Biophys Res Commun***412**, 373-378, doi:10.1016/j.bbrc.2011.07.105 (2011).

24 Liu J., Wang D., Chen Y., Sun H., He S., Wang C. *et al.* 1H NMR-based metabonomic analysis of serum and urine in a nonhuman primate model of diabetic nephropathy. *Mol Biosyst***9**, 2645-2652, doi:10.1039/c3mb70212j (2013).

25 Kanwar Y. S., Sun L., Xie P., Liu F. Y. & Chen S. A glimpse of various pathogenetic mechanisms of diabetic nephropathy. *Annu Rev Pathol***6**, 395-423, doi:10.1146/annurev.pathol.4.110807.092150 (2011).

26 Moghadasali R., Azarnia M., Hajinasrollah M., Arghani H., Nassiri S. M., Molazem M. *et al.* Intra-renal arterial injection of autologous bone marrow mesenchymal stromal cells ameliorates cisplatin-induced acute kidney injury in a rhesus Macaque mulatta monkey model. *Cytotherapy***16**, 734-749, doi:10.1016/j.jcyt.2014.01.004 (2014).

27 Moghadasali R., Hajinasrollah M., Argani H., Nassiri S. M., Najarasl M., Sodeifi N. *et al.* Autologous transplantation of mesenchymal stromal cells tends to prevent progress of interstitial fibrosis in a rhesus Macaca mulatta monkey model of chronic kidney disease. *Cytotherapy***17**, 1495-1505, doi:10.1016/j.jcyt.2015.06.006 (2015).

28 Chabardes-Garonne D., Mejean A., Aude J. C., Cheval L., Di Stefano A., Gaillard M. C. *et al.* A panoramic view of gene expression in the human kidney. *Proc Natl Acad Sci U S A***100**, 13710-13715, doi:10.1073/pnas.2234604100 (2003).

29 Lee J. W., Chou C. L. & Knepper M. A. Deep Sequencing in Microdissected Renal Tubules Identifies Nephron Segment-Specific Transcriptomes. *J Am Soc Nephrol***26**, 2669-2677, doi:10.1681/ASN.2014111067 (2015).

30 Shankland S. J., Smeets B., Pippin J. W. & Moeller M. J. The emergence of the glomerular parietal epithelial cell. *Nat Rev Nephrol***10**, 158-173, doi:10.1038/nrneph.2014.1 (2014).

31 Habuka M., Fagerberg L., Hallstrom B. M., Kampf C., Edlund K., Sivertsson A. *et al.* The kidney transcriptome and proteome defined by transcriptomics and antibody-based profiling. *PLoS One***9**, e116125, doi:10.1371/journal.pone.0116125 (2014).

32 Stuart T., Butler A., Hoffman P., Hafemeister C., Papalexi E., Mauck W. M., 3rd *et al.* Comprehensive Integration of Single-Cell Data. *Cell***177**, 1888-1902 e1821, doi:10.1016/j.cell.2019.05.031 (2019).

33 Devuyst O. & Pattaro C. The UMOD Locus: Insights into the Pathogenesis and Prognosis of Kidney Disease. *J Am Soc Nephrol***29**, 713-726, doi:10.1681/ASN.2017070716 (2018).

34 Markadieu N. & Delpire E. Physiology and pathophysiology of SLC12A1/2 transporters. *Pflugers Arch***466**, 91-105, doi:10.1007/s00424-013-1370-5 (2014).

35 Durinck S., Spellman P. T., Birney E. & Huber W. Mapping identifiers for the integration of genomic datasets with the R/Bioconductor package biomaRt. *Nat Protoc***4**, 1184-1191, doi:10.1038/nprot.2009.97 (2009).

36 Kaushal D., Mehra S., Didier P. J. & Lackner A. A. The non-human primate model of tuberculosis. *J Med Primatol***41**, 191-201, doi:10.1111/j.1600-0684.2012.00536.x (2012).

37 Amedee A. M., Nichols W. A., Robichaux S., Bagby G. J. & Nelson S. Chronic alcohol abuse and HIV disease progression: studies with the non-human primate model. *Curr HIV Res***12**, 243-253, doi:10.2174/1570162x12666140721115717 (2014).

38 Marmion D. J. & Kordower J. H. alpha-Synuclein nonhuman primate models of Parkinson's disease. *J Neural Transm (Vienna)***125**, 385-400, doi:10.1007/s00702-017-1720-0 (2018).

39 Haque R. U. & Levey A. I. Alzheimer's disease: A clinical perspective and future nonhuman primate research opportunities. *Proc Natl Acad Sci U S A*, doi:10.1073/pnas.1912954116 (2019).

40 Ruan Q. W., Yu Z. W. & Ma Y. X. [Aging and aging intervention by coloric restriction in nonhuman primate rhesus monkeys]. *Sheng Li Ke Xue Jin Zhan***44**, 6-11 (2013).

41 Pound L. D., Kievit P. & Grove K. L. The nonhuman primate as a model for type 2 diabetes. *Curr Opin Endocrinol Diabetes Obes***21**, 89-94, doi:10.1097/MED.0000000000000043 (2014).

42 Huang L., Liao J., He J., Pan S., Zhang H., Yang X. *et al.* Single-cell profiling reveals sex diversity in human renal proximal tubules. *Gene***752**, 144790, doi:10.1016/j.gene.2020.144790 (2020).

Figures

Figure 1

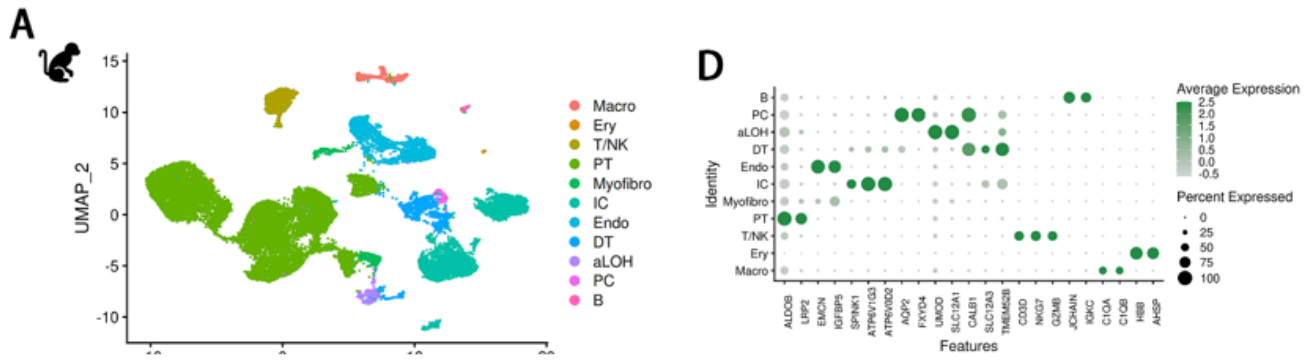

Figure 1

scRNA-seq atlas for cynomolgus monkey, human and mouse kidney cells. (A, B and C) UMAP plot showing the unbiased classification of cynomolgus monkey, human and mouse kidney cells. (D, E and F) Dot plot showing the marker genes of each cluster in cynomolgus monkey, human and mouse kidney. Dot size represents the proportion of cells within the cluster expressing each transcriptome, and dot color corresponds to expression levels. PT: proximal tubule, ICs: intercalated cell, PCs: principle cells, Endo: endothelial, DT: distal cell, Macro: macrophage, aLOH: ascending loop of Henle, B: B lymphocyte, T/NK: T lymphocyte and natural killer cell, Myofibro: myofibroblast, Ery: erythroid, Plasma: plasma cell, Neutro: neutrophil.

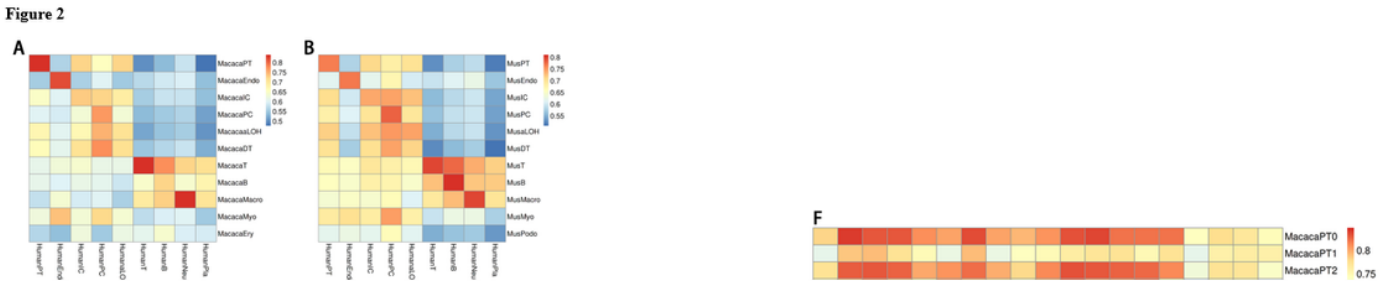

Figure 2

Comparison of gene expression of cynomolgus monkey, human and mouse kidney. (A) Heatmap indicates the Pearson correlations on the averaged gene profiles in each cell type of human (vertical) and monkey kidney (horizontal). (B) Heatmap indicates the Pearson correlations on the averaged gene profiles in each cell type of human (vertical) and mouse (horizontal) kidney. (C) Scatterplot shows the homologous genes, with the average expression in total cells in human (vertical) and monkey (horizontal) kidney tissues. Genes with distinct DEGs are labeled. The Pearson correlation coefficient was 0.806 (R). The blue lines are the regression curves. (D) Scatterplot shows the homologous genes, with the average expression in total cells in human (vertical) and mouse (horizontal) kidney tissues. Genes with distinct DEGs are labeled. The Pearson correlation coefficient was 0.78 (R). The blue lines are the regression curves. (E) Scatterplot shows the homologous genes, with the average expression in proximal tubule cells in human (vertical) and monkey (horizontal) kidney. Genes with distinct DEGs are labeled. The Pearson correlation coefficient was 0.78 (R). The blue lines are the regression curves. (F) Heatmap shows the Pearson correlations on the averaged gene profiles among each subsets of PT cells in human (vertical) and monkey (horizontal).

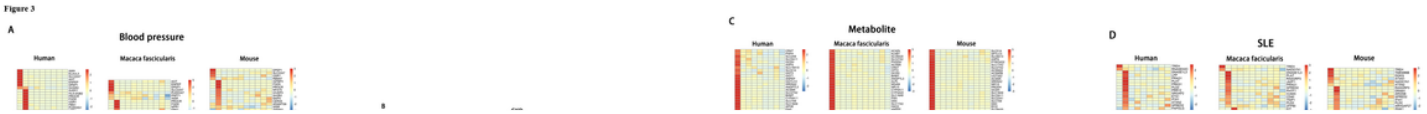

Figure 3

Cell-type specific expression of GWAS-identified complex traits renal disease genes. (A-D) Averaged expression of genes was calculated in each cell type. The color scheme is based on z-score. In the heatmap, each row represents one gene and each column is single cell type.

Figure 4

The expression of therapeutic genes related to hypertension in different species. (A-C) The distribution and expression of target genes associated with therapy in hypertension across species. (Human (A), Cynomolgus monkey (B), Mouse (C))

Supplementary Files

This is a list of supplementary files associated with this preprint. Click to download.

- AdditionalfileData1.xlsx
- AdditionalfileFig1.pdf
- AdditionalfileFig2.pdf